



# Observations of Atmospheric Chemical Deposition to High Arctic Snow

Katrina M. Macdonald<sup>1</sup>, Sangeeta Sharma<sup>2</sup>, Desiree Toom<sup>2</sup>, Alina Chivulescu<sup>2</sup>, Sarah Hanna<sup>2</sup>, Allan Bertram<sup>2</sup>, Andrew Platt<sup>2</sup>, Mike Elsasser<sup>2</sup>, Lin Huang<sup>2</sup>, Nathan Chellman<sup>3</sup>, Joseph R. McConnell<sup>3</sup>, Heiko Bozem<sup>4</sup>, Daniel Kunkel<sup>4</sup>, Ying Duan Lei<sup>1</sup>, Greg J. Evans<sup>1</sup>, Jonathan P. D. Abbatt<sup>5</sup>

<sup>1</sup>Department of Chemical Engineering and Applied Chemistry, University of Toronto, M5S 3E5, Canada

<sup>2</sup>Climate Research Division, Environment and Climate Change Canada, Toronto, M3H 5T4, Canada

<sup>3</sup>Desert Research Institute, Reno, 89512, United States of America

<sup>4</sup>Institute for Atmospheric Physics, Johannes Gutenberg University Mainz, Becher Weg, 21 55128, Germany

10 <sup>5</sup>Department of Chemistry, University of Toronto, M5S 3H6, Canada

*Correspondence to:* Jonathan Abbatt ( jabbatt@chem.utoronto.ca)

**Abstract.** Rapidly rising temperatures and loss of snow and ice cover have demonstrated the unique vulnerability of the high Arctic to climate change. There are major uncertainties in modelling the chemical depositional and scavenging processes of Arctic snow. To that end, fresh snow samples collected on average every four days at Alert, Nunavut, from September 2014 to June 2015 were analyzed for black carbon, major ions, and metals, and their concentrations and fluxes reported. Comparison with simultaneous measurements of atmospheric aerosol mass loadings yields effective deposition velocities which encompass all processes by which the atmospheric species are transferred to the snow. It is inferred from these values that dry deposition is the dominant removal mechanism for several compounds over the winter while wet deposition increased in importance in the fall and spring, probably due to enhanced scavenging by mixed-phase clouds. Black carbon aerosol was the least efficiently deposited species to the snow. These measurements are a unique data set for comparison to models that incorporate deposition to high Arctic snow.

## 1 Introduction and Background

In recent decades drastic changes have been observed within the Arctic, including a rapid increase in surface temperatures and loss of sea ice and snow cover (Rigor et al., 2000; Stroeve et al., 2005; Hartmann et al., 2013). Not only have these changes had adverse consequences for local populations and ecosystems, it has been suggested that their global impacts may be significant (Law and Stohl, 2007; AMAP, 2011). Specifically, light-absorbing compounds, the most widely-studied of which being black carbon (BC) particles, can have a particularly significant impact on the Arctic atmosphere and snow systems through the absorption of solar radiation and subsequent warming and snow melt (Bond et al., 2013). While the Arctic atmosphere has been previously explored spatially, temporally, and compositionally (e.g., Hartmann et al., 2013), Arctic snow and the mechanisms linking snow to the atmosphere have been the subject of only a relatively small number of studies (AMAP, 2011), despite the enormous amount of research conducted on the Arctic Haze phenomenon (Quinn et al.,



2007). Observations of fresh snow samples are particularly uncommon and previous explorations of snow deposition and scavenging mechanisms have been largely reliant on aged snowpack sampling, modelling, and laboratory tests.

Aerosols entering the Arctic atmosphere, either generated locally or transported from elsewhere, can be removed by atmospheric transport or deposition. Deposition of particles follows two mechanisms: dry deposition, whereby particles are deposited to the ground by impaction, gravitational settling, and Brownian motion; and wet deposition, whereby particles are scavenged by hydrometeors and deposited through precipitation. Wet deposition is further split into two scavenging mechanisms: in-cloud scavenging which removes particles from the cloud layer during precipitation formation, and below-cloud scavenging which removes particles from the atmospheric column through which precipitation falls. Gaseous compounds also undergo similar scavenging processes (Seinfeld and Pandis, 2006).

10 The rate of dry deposition is dependent on the properties of the depositing particle, the surface onto which deposition occurs, and the air-surface boundary layer (Sehmel, 1980; Zhang and Vet, 2006). Dry deposition velocities of accumulation mode particles, the dominant mass-weighted mode of particles observed in the non-summer Arctic (Sharma et al., 2013), to snow have been modelled and observed over a range of 0.01 to 0.60 cm/s, typically within 0.02 to 0.10 cm/s; gaseous deposition velocities to a snow surface shows a similar range, with observations from 0.05 to 0.50 cm/s and a typical velocity of approximately 0.10 cm/s (McMahon and Denison, 1979; Sehmel, 1980; Davidson et al., 1987; Hillamo et al., 1993; Petroff and Zhang, 2010). Wet deposition is dependent on the properties of the depositing aerosol and the atmospheric conditions. In-cloud scavenging is largely controlled by a particle's size and composition which dictate its ability to nucleate hydrometeors and to be scavenged by cloud droplets. Particles can act as cloud condensation nuclei (CCN) that nucleate water droplets or ice nuclei (IN) that nucleate ice crystals. Common CCN components include sea salt, sulphate ( $\text{SO}_4^{2-}$ ), and nitrate ( $\text{NO}_3^-$ ), while mineral dust and bioaerosols are common IN (Hoose and Möhler, 2012; Farmer, Cappa, and Kreidenweis, 2015). Typically, BC is considered to be an ineffective CCN or IN (Hoose and Möhler, 2012; Farmer, Cappa, and Kreidenweis, 2015). Although liquid water clouds are not expected during the Arctic winter, mixed-phase clouds, which contain both liquid water and ice, have been observed in this region at temperatures well below 0 °C, in unusual cases down to -40 °C but more commonly between -20 °C and -10 °C (Morrison et al., 2005; Shupe et al., 2006). Below-cloud deposition is dependent snow type and meteorological conditions, which dictate the volume of air scavenged per snowfall (Zhang and Vet, 2006). Particle size also affects below-cloud scavenging with higher scavenging efficiencies for particles above 2.5 µm diameter relative to accumulation mode particles (Zhang and Vet, 2006). The efficiencies of below-cloud scavenging of gases and particles can be similar at an order of magnitude level, though measurements of gaseous scavenging in particular are infrequent and dependent on composition (McMahon and Denison, 1979). The total wet deposition is a function of the volume of precipitation. Hence, wet deposition is not typically described via a deposition velocity.

The goals of this paper are to present a new dataset in which the chemical composition of freshly fallen snow was measured through a fall-winter-spring period at a high Arctic field station. By combining these data with simultaneous measurements of ambient aerosol, the efficiency of deposition of individual species from the atmosphere to the snow can be evaluated under a set of broad assumptions. While this paper presents the measurement data set in detail and focuses on the



depositional and scavenging mechanisms that can be inferred from it, a subsequent publication will identify potential pollutant sources based on the snow compositional data. To our knowledge, this is the first time that the composition of freshly fallen snow has been analyzed at high temporal frequency throughout an entire cold season in the high Arctic.

## 2 Methodology

### 5 2.1 Snow Sample Collection

Snow samples were collected at Environment and Climate Change Canada's (ECCC) Dr. Neil Trivett Global Atmosphere Watch Observatory at Alert, Nunavut from September 14<sup>th</sup>, 2014 to June 1<sup>st</sup>, 2015 as part of the Network on Climate and Aerosols Research (NETCARE) initiative to create a temporally-refined and broadly speciated dataset of high Arctic snow measurements. Alert is a remote outpost in the Canadian high Arctic, at the northern coast of Ellesmere Island (82°27' N, 10 62°30' W), with a small transient population of research and military personnel (location details provided in supplemental Sect. S3). Snow samples were collected from two Teflon-surfaced snow tables (about 1 m<sup>2</sup> by 1 m above ground level, shown in supplemental Figure S2) located in an open-air minimal traffic site, about 6 km SSW of the Alert base camp, 201 m above sea level. Freshly fallen snow was collected from the tables using a Teflon scraper and scoop by dividing the table into rectangular portions for replicate sample collection. Four replicate samples were collected for this study and the table 15 area cleared to fill each bottle was recorded. Prior to their first use and between snow sample collections, both snow tables were fully cleared of all remaining snow and cleaned with methanol. Samples were collected as soon after the end of each snowfall as feasible, conditions allowing. From September 14<sup>th</sup>, 2014 to June 1<sup>st</sup>, 2015, 59 sets of snow samples were collected. The interval between collections varied based on snowfall frequency, ranging from 1 to 19 days with an average of 4 days. The table area and collection period length associated with each sample allowed the measured concentration of each 20 analyte to be converted to a flux. This ability to assign a precise deposition area and time period to each sample, minimizing the inaccuracies introduced by extensive snow redistribution by winds or snow sublimation/melt, was a considerable advantage over previous sampling campaigns of aged snowpack.

New sample bottles were used for the collection campaign and each bottle was thoroughly cleaned prior to use. Bottles and lids were soaked in 5% nitric acid, 1% detergent in water (Alconox), and deionized 18.2 MΩ water (DIW), allowing 10 to 14 25 hours for each soak. Each dried bottle was then sealed in a protective plastic sleeve until use. At Alert, plastic outer gloves and lab coats were used to minimize contamination during collection, and the scraper and scoop were cleaned with DIW prior to each collection. Alert station operators also recorded the collection conditions for each sample. Atypical snowfall events were noted: diamond dust events, small crystalline snowfalls; and blowing snow events, periods when high winds potentially resuspended snow from the ground. Operators also made note of any unusual weather conditions such as fog or 30 blizzard conditions. Local meteorological conditions were monitored by the Alert ECCC stations (Climate IDs 2400306, 2400305, and 2400302) (retrieved Nov. 2015 from [climate.weather.gc.ca](http://climate.weather.gc.ca)).



## 2.2 Snow Sample Preparation and Analysis

A broad suite of analytes was quantified using replicate snow samples from each snowfall: BC, major ions, and metals. The procedures for BC and major ion analysis followed well developed protocols and are described only briefly herein, but the methodology developed for metals quantification is described in greater detail. All snow samples were kept frozen prior to analysis, throughout storage and shipping.

Refractory BC quantification was completed via single-particle soot photometry (SP2) at the Desert Research Institute, Reno, Nevada, as per McConnell et al. (2007). Briefly, snow samples collected in 50 mL Pyrex bottles were melted at room temperature the morning of analysis and sonicated for 1 minute. Each sample was atomized via Apex-Q nebulizer and dried particles with 0.02 to 50 fg BC were quantified. Observed BC mass distributions did not suggest significant underestimation of the total BC mass due to this size cut-off, (Macdonald, 2016). A quality control standard and analysis blank were analyzed for every batch of 17 samples.

Major ions were measured via ion chromatography (IC) at ECCC, Toronto office, as per Toom-Sauntry and Barrie (2002). Briefly, samples collected in 250 mL high-density polyethylene (HDPE) bottles were melted in a warm water bath. Shortly after melting, ions were quantified using a Dionex IC (DX600 for anions and cations, ICS2000 for organic acids) with a 200  $\mu$ L sample loop. Aliquots of these samples were also used for pH analysis (Denver pH analyzer). Equipment was calibrated daily and quality control runs completed every ten samples.

Metals analysis was completed via inductively coupled plasma mass spectrometry (ICP-MS) at the University of Toronto. Samples collected in 500 mL HDPE bottles were melted rapidly in a microwave oven and immediately filtered with a 13 mm diameter 0.45  $\mu$ m cellulose acetate filter (Whatman) using a reusable polytetrafluoroethylene filter holder (Sartorius) and a polyethylene syringe (BD). The full collected volume was filtered for each sample, ranging from 40 to 200 mL meltwater. Both filtrate and filter were analyzed and considered as soluble and insoluble metals, respectively. Samples were digested using 70% nitric acid ( $\text{HNO}_3$ ), ultra-trace grade (SCP Science PlasmaPure). Filtrate samples were digested by bringing the solution to 2%  $\text{HNO}_3$  mass/mass; however, filter samples required an augmented digestion procedure to enable quantification. It has been shown that microwave digestion significantly improves the recovery of insoluble metals without the need for more hazardous digestion reagents (Swami et al., 2001; Pekney and Davidson, 2005; US EPA, 2007). Each cellulose filter was placed in a polytetrafluoroethylene microwave digestion tube (CEM MARSXpress) with ultra-trace grade 70%  $\text{HNO}_3$ . Filtrate and filter were sealed and left overnight at room temperature to digest. After a 10 to 15 hr digestion time, DIW was added to each filter vessel to dilute the solution to 2%  $\text{HNO}_3$ . The filter samples were then placed in a microwave digester (CEM MARS 6) and digested using the US Environmental Protection Agency (US EPA) 3051 procedure for trace metal analysis. The digested filter solutions were transferred to polypropylene tubes and centrifuged to separate any undigested residue. An average mass recovery precision of  $\pm 1.5\%$  was observed over the digestion procedure. Filter and filtrate samples were analyzed by ICP-MS (Thermo Scientific iCAP Q) under kinetic energy discrimination mode. Dwell times were set to 0.02 s for analytes with an ionization potential less than 9 eV and 0.10 s for analytes with a greater



ionization potential. The wash time was set to 75 s and uptake time to 50 s (as per Henry and Wills, 2012; Wang and Miao, 2016). A performance test and calibration (SCP Science PlasmaCAL QC Std 4) were completed prior to each run, and quality control checks were completed every ten samples to quantify instrument drift. All concentrated standards were followed by an extra DIW blank to prevent extensive carry-over from standard to samples. An internal standard, selected so as to minimize interference with measured analytes while covering the full analyzed spectrum of mass to charge ratios, was included to quantify and correct for any instrument drift or inter-sample variability (SCP Science Int. Std. Mix 1). The full 4.6 to 245 mass/charge ratio ( $m/z$ ) range was scanned and, where necessary, interference corrections were applied (as per Henry and Wills, 2012; Wang and Miao, 2016). It should be noted that this preparation and analysis procedure is not expected to retain highly volatile metals, such as Hg. All apparatus components were thoroughly cleaned before and between uses with  $\text{HNO}_3$  and DIW. The microwave digestion vessels underwent a full digestion cycle with 15 mL 70%  $\text{HNO}_3$  and then were rinsed with ultra-trace grade  $\text{HNO}_3$  and DIW prior to each use. All sample preparation was completed in class 100 vertical laminar flow cabinet (AirClean Systems AC 632).

Quality assurance is of the utmost importance in the analysis of dilute Arctic samples. Instrument accuracy was confirmed through the analysis of certified reference materials. The uncertainty of each measurement was estimated based on analysis detection limits and reproducibility (as per Reff et al., 2007; Norris et al., 2014). Also, the signal-to-noise (S/N) of each analyte was calculated to indicate the strength of each measurement (as per Norris et al., 2014). A S/N over 2 was considered to be strong (Paatero and Hopke, 2003). Regular analysis of blanks was used for background subtraction and to define method detection limits (MDL) as three standard deviations of the blank levels. Beyond typical preparation blanks, which used DIW in the place of snow melt water, field blanks were also analyzed. Once per month, a set of empty sample bottles was taken to the snow table, opened, and resealed without collection. These field blank bottles were stored and shipped with the regular samples and rinsed with DIW to quantify any contamination throughout the sampling process. Any influence from the local Alert base camp was identified using local wind records and the activity logs of the base camp personnel. The only analytes that showed a potential influence from base camp winds were crustal metals, with Pearson's correlation coefficients ( $R$ ) of 0.4 to 0.6 ( $p$ -value 0.0001 to 0.002) between snow mixing ratios and periods of base camp winds. Base camp combustion activity logs showed no significant impact on the samples. Additional methodology details are provided in Macdonald (2016).

### 2.3 Atmospheric Monitoring

Ground-level atmospheric monitoring data from the Alert Global Atmospheric Watch Observatory were provided by ECCC. Atmospheric BC was monitored hourly by SP2 (Droplet Measurement Technology) (as per Schroder et al., 2015) and major ions by IC of 6 to 8-day high-volume filters of total suspended particles (Hi-Vol) (as per Sirois and Barrie, 1999). Both the SP2 and Hi-Vol were operational throughout the campaign with coverages of 92% and 94%, respectively. As for the snow SP2 analysis, the influence of BC particle size cut-off limits was considered but found to have minimal impact, especially when considered at a monthly scale.



## 2.4 Transport Modelling

The Lagrangian particle dispersion model FLEXPART (Stohl et al., 2005) was used to determine the source region of air masses that were measured over Alert. This model has previously been shown to be an effective tool for the prediction of transport pathways into and within the Arctic (e.g., Paris et al., 2009). The simulations were driven using meteorological analysis data from the European Centre for Medium-Range Weather Forecasts with a horizontal grid spacing of 0.25° in longitude and latitude and 137 levels in the vertical. For each 5 day period during the measurement period we released tracers over Alert in four different altitude levels, 100 m, 500 m, 1000 m, and 2000 m above sea level, to distinguish between the levels which may be scavenged by snow. The tracers were then traced for ten days backward to obtain the source region for the particular time period.

## 10 3 Results and Discussion

### 3.1 Total Deposition of Arctic Snowfall Events

Unlike traditional snowpack collection campaigns, each sample for this study was collected fresh after a known time and over a known area. Given that the snow tables were exposed to the ambient atmosphere for the entirety of each collection period, the measured deposition is considered to represent the total deposition (wet and dry) for said period. There are two caveats to this assumption. Firstly, dry deposition at the beginning of each period would fall directly on the exposed clean table rather than onto previously deposited snow. The difference in surface characteristics created unknown uncertainty in the deposition rate and collection efficiency of the initial portion of dry deposition compared to that which deposited onto a snow-covered table. Secondly, strong winds can disturb and redistribute the snowpack and cause snow to be blown off and/or onto the snow table. Alert operators recorded four occasions when the snowpack was observed to be resuspended due to high winds and these were excluded from the presented results. Several additional collection periods saw larger snow depths measured by local meteorological stations than that observed on the collection table, implying snow loss from the table. However, as the meteorological station was over 1 km away from the collection site and about 50 m lower in elevation, it was unclear whether this disagreement was the result of snow loss from the snow table or the natural spatial variability in precipitation. Thus, no correction was applied to the collected data based on the meteorological station's snow depth.

The observed snow mixing ratios and fluxes are summarized in Table 1 and Figure 1 for measured analytes with a strong S/N. Mixing ratio is reported as parts per billion by mass (ppb) with the exception of pH. Flux is reported on a per day basis to take into account the differing collection period lengths; however, it should be noted that this length corresponds to the entire collection period (i.e., the number of days between clearing the snow table), not just the length of time when snow was actually falling. A full record of the measured deposition over the campaign is provided in the supplemental (Table S1-6) along with the associated uncertainties and values specific to atypical collection conditions. It should be noted that although





IC measurements are provided as the measured ions throughout the discussion, these analytes may not necessarily exist in the free form in the environment. Also, the metal measurements provided in Table 1 are total values, insoluble and soluble. The soluble fractions differed by analyte and by date and are provided in the supplemental (Table S4-6). Comparison of the measured mean values with previous snow observations by others provided a general corroboration of the measurements (see supplemental Table S7 for details); however, given the limitations of previous snow measurements as discussed above, no extensive comparison of seasonal trends could be conducted.

**Table 1: Overview of fresh snow composition and inferred fluxes over the 2014-15 winter season.**

| Analysis         | Analyte                                     | Snow Mixing Ratio (ppb)        |                                |                                | Snow Flux ( $\mu\text{g}/\text{m}^2/\text{d}$ ) |                                |                                |
|------------------|---|--------------------------------|--------------------------------|--------------------------------|---|--------------------------------|--------------------------------|
|                  |   | 25 <sup>th</sup><br>Percentile | 50 <sup>th</sup><br>Percentile | 75 <sup>th</sup><br>Percentile | 25 <sup>th</sup><br>Percentile                  | 50 <sup>th</sup><br>Percentile | 75 <sup>th</sup><br>Percentile |
| SP2              | BC  | 1.3                            | 2.3                            | 4.1                            | 0.24  | 0.42                           | 0.86                           |
| IC               | MSA   | <1.9                           | <1.9                           | 2.5                            | <0.1  | <0.1                           | <0.1                           |
|                  | ACE   | 9.6                            | 19.9                           | 27.3                           | 1.9   | 3.5                            | 7.5                            |
|                  | PRP   | <1.5                           | 2.2                            | 5.3                            | <0.10   | 0.62                           | 2.06                           |
|                  | FOR   | 8.4                            | 11.0                           | 14.8                           | 1.32  | 2.66                           | 4.72                           |
|                  | Cl <sup>-</sup>                             | 132                            | 249                            | 605                            | 35.6  | 59.2                           | 122.5                          |
|                  | Br <sup>-</sup>                             | <5.0                           | <5.0                           | 12.1                           | <0.3  | <0.3                           | 2.0                            |
|                  | NO <sub>3</sub> <sup>-</sup>                | 85.4                           | 152.5                          | 265.8                          | 10.8  | 23.8                           | 50.2                           |
|                  | SO <sub>4</sub> <sup>2-</sup>               | 204                            | 297                            | 554                            | 32.4  | 69.9                           | 132.5                          |
|                  | C <sub>2</sub> O <sub>4</sub> <sup>2-</sup> | <18.0                          | <18.0                          | 20.8                           | <1.2  | 0.2                            | 2.7                            |
|                  | Na <sup>+</sup>                             | 55.4                           | 110.7                          | 237.9                          | 10.9  | 20.1                           | 52.4                           |
|                  | NH <sub>4</sub> <sup>+</sup>                | 10.6                           | 12.4                           | 16.6                           | 1.3   | 2.5                            | 5.9                            |
|                  | K <sup>+</sup>                              | 8.0                            | 15.4                           | 23.5                           | 0.8   | 2.0                            | 3.9                            |
| Mg <sup>2+</sup> | 22.3  | 43.3                           | 77.4                           | 2.2                            | 7.6   | 13.3                           |                                |
| Ca <sup>2+</sup> | <133.1                                      | 193.1                          | 409.2                          | <9.1                           | 14.6  | 51.5                           |                                |
| pH               | H <sup>+</sup>                              | 1.39                           | 4.25                           | 6.97                           | 0.25  | 0.88                           | 1.87                           |
| Analyzer         | pH  | 5.16                           | 5.37                           | 5.86                           | n/a   | n/a                            | n/a                            |
| ICP-MS           | Mg  | 18.2                           | 28.6                           | 67.6                           | 3.0   | 6.5                            | 14.5                           |
|                  | Al  | <3.2                           | 7.2                            | 19.2                           | <0.2  | 1.4                            | 3.3                            |
|                  | V   | 0.006                          | 0.012                          | 0.086                          | 0.002   | 0.003                          | 0.014                          |
|                  | Mn  | 0.23                           | 0.64                           | 1.14                           | 0.06  | 0.10                           | 0.20                           |
|                  | Fe  | 3.6                            | 10.8                           | 29.1                           | 0.5   | 2.0                            | 3.9                            |
|                  | Co  | <0.002                         | 0.004                          | 0.011                          | <0.0002   | 0.0007                         | 0.0015                         |
|                  | Cu  | <0.02                          | 0.05                           | 0.28                           | 0.001   | 0.010                          | 0.053                          |
|                  | As  | 0.007                          | 0.044                          | 0.071                          | 0.002   | 0.006                          | 0.013                          |
|                  | Se  | 0.010                          | 0.024                          | 0.058                          | 0.002   | 0.004                          | 0.010                          |
|                  | Sb  | 0.004                          | 0.010                          | 0.018                          | 0.001   | 0.002                          | 0.004                          |
|                  | Tl  | <0.0001                        | 0.0001                         | 0.0004                         | <7.2×10 <sup>-6</sup>                           | 15.6×10 <sup>-6</sup>          | 54.0×10 <sup>-6</sup>          |
| Pb               | 0.05  | 0.25                           | 0.41                           | 0.012                          | 0.039   | 0.086                          |                                |

Notes: MSA = methanesulphonate; ACE = acetate; PRP = propionate; FOR = formate, C<sub>2</sub>O<sub>4</sub><sup>2-</sup> = oxalate; NH<sub>4</sub><sup>+</sup> = ammonium. < # indicates measurement is below MDL.

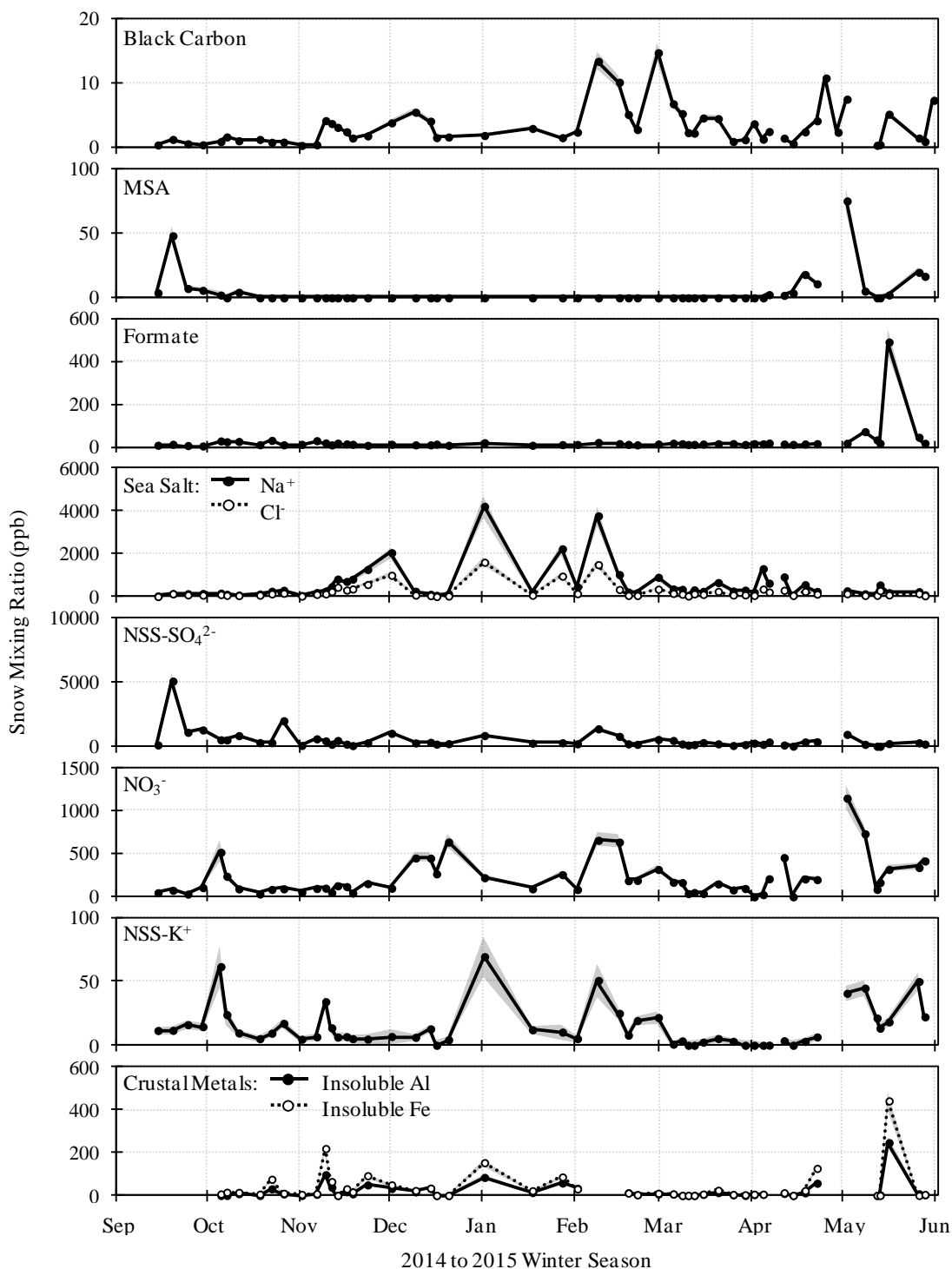


Figure 1: Measured snow mixing ratio (line) and uncertainty (shaded area) of key analytes over 2014 to 2015 campaign.





## 3.2 Factors Influencing Snow Scavenging and Deposition

### 3.2.1 Effective Deposition Velocity

A simplistic model for flux, Eq. (1), was used to describe the measured deposition:

$$F_S^{ij} = C_A^{ij} v_d^{ij}, \quad (1)$$

5 where  $F_S^{ij}$  is the flux deposited to snow of the  $j^{\text{th}}$  analyte over the  $i^{\text{th}}$  period;  $C_A^{ij}$  is the arithmetic average atmospheric concentration; and  $v_d^{ij}$  is the effective deposition velocity.

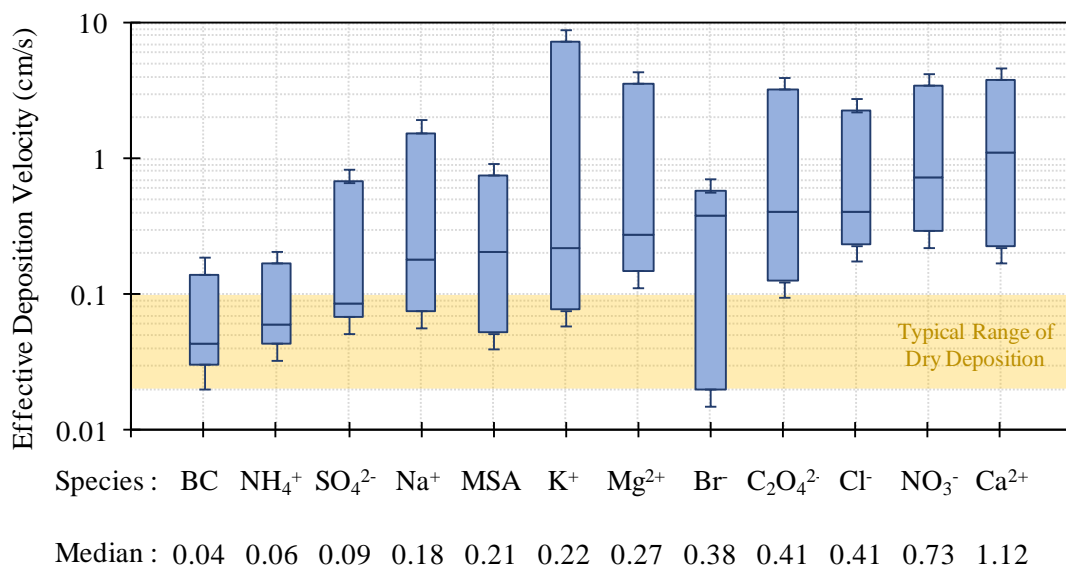
The measured flux ( $F_S$ ) represents the total deposition by wet and dry mechanisms. Thus, the effective deposition velocity ( $v_d$ ) encompasses the variety of aerosol and meteorological properties controlling deposition efficiency and the relative importance of each deposition pathway: dry, wet in-cloud, and wet below-cloud scavenging. The three deposition  
10 mechanisms relate to different atmospheric concentrations, a gradient which is not necessarily captured when the ground-level atmospheric concentration ( $C_A$ ) is used to calculate the effective deposition velocity: dry deposition affects the lower atmosphere, in-cloud scavenging the cloud layer, and below-cloud scavenging the full below-cloud atmospheric column. So, the calculated velocities have an intrinsic variability dependent on the vertical atmospheric profile of each analyte. Previous observations of vertical profiles in the Arctic have shown a great degree of variability with altitude, but typically within the  
15 below-cloud layer (the lower 2-4 km) atmospheric concentrations are more consistent (Leitch et al., 1989; Spackman et al., 2010; Sharma et al., 2013). As well, in NETCARE aircraft measurements yet to be published, it was shown through SP2 and aerosol mass spectrometry measurements of aerosol composition from the ground to 3 km altitude during April, 2015 that little vertical variability was apparent in aerosol BC,  $\text{SO}_4^{2-}$ ,  $\text{NO}_3^-$ , and ammonium ( $\text{NH}_4^+$ ). Thus, the use of ground-level measurements was considered acceptable. An overview of measured atmospheric concentrations is provided in the  
20 supplemental (Table S8).

The ratio of monthly total snow flux to monthly-averaged ground-level atmospheric concentrations was used for the calculation of effective deposition velocities. The use of monthly values allowed for intra-monthly variability in deposition conditions, such as snow type and snow/air interface properties which were not explicitly monitored and would complicate analysis of deposition over individual snowfall events. Thus, the range of calculated effective deposition velocities of an  
25 analyte describes their general deposition regime, capturing the impacts of any parameters which led to seasonal changes in the predominant deposition mechanisms directly or through changes in aerosol aging. A monthly analysis also provides for better future comparisons with modelled results which would not replicate individual events.

The calculated monthly effective deposition velocities are summarized in Figure 2 for analytes measured both in fresh snow (via SP2 and IC) as well as in the ground-level atmosphere (via SP2 and Hi-Vol filters). Median effective deposition  
30 velocities ranged from 0.04 to 1.1 cm/s. January and February velocities were excluded from median calculation because blizzard and high wind conditions were believed to have caused significant losses of snow from the snow tables during these months (based on operator reports and larger snow depths measured at local meteorological stations), which would lead to underestimation of the snow flux for these months. Since wet deposition is a function of precipitation volume, the effective



deposition velocity is comparable only across periods of equal total precipitated volume. With the exception of January and February, 2015, the total monthly snow precipitation over the campaign was relatively constant, with a relative standard deviation of 20%. Error bars in Figure 2 describe the combined uncertainty of the snow and atmospheric measurements.



5 **Figure 2: Effective deposition velocities.** Columns show the calculated minimum, median, and maximum monthly effective deposition velocities over the sampling campaign, excluding January and February, 2015. Error bars show uncertainty of deposition velocities. Typical range of dry deposition velocity for accumulation mode particles to snow by others (Davidson et al., 1987; Petroff and Zhang, 2010).

The range of calculated effective deposition velocities was compared to the expected range of dry deposition velocities for  
10 typical accumulation mode Arctic particles, 0.02 to 0.10 cm/s (Davidson et al., 1987; Petroff and Zhang, 2010), as highlighted in Figure 2. The calculated effective velocities fell within or above the dry deposition range, indicating dry deposition may be the dominant deposition mechanism in some measurements while others show enhanced deposition with an increased influence of wet deposition processes.

### 3.2.2 Variation in Deposition by Composition

15 Deposition efficiency is dependent on the properties of the aerosol being deposited. The calculated monthly effective deposition velocities showed a relative standard deviation of 60 to 150% across the measured analytes, while measurement-based uncertainty was estimated as only  $\pm 35\%$ , indicating a significant impact of aerosol state or properties on deposition. This variability could be the result of variations in aerosol phase and/or particle size, shape, and cloud nucleation affinity. The only size-resolved speciated analysis available to this study was SP2; however, the mass diameters estimated by SP2 do  
20 not provide information on the aerodynamic diameter which is of greater concern in deposition processes. Furthermore, it could not be known if BC size distribution in the snow samples was maintained over sample melt and sonication prior to analysis. Without additional information, the impact of size and shape on deposition could not be inferred from this study



beyond simple deductions based on the typical particle sizes associated with aerosol types. Similarly, due to a lack of information, the possible impact of particle coating was not addressed. The observed differences in deposition are therefore primarily discussed in the context of phase state and cloud nucleation affinity.

Due to the nature of the Hi-Vol analysis, the measured atmospheric concentrations include only the particle-phase ambient species; however, snow can scavenge both the particle and gas phases, and thus snow samples provide a composite measurement of both. The measurement of sea salt species was used as a case study to illustrate the impact of particle/gas-phase partitioning. The two dominant components of sea salt, Na and Cl, were measured both in snow samples (IC) and in the atmosphere (Hi-Vol). Previous studies have found Na and Cl observed within the Arctic to be predominantly marine in origin (Sirois and Barrie, 1999; Nguyen et al., 2013). This marine origin is supported by the excellent correlation of Na and Cl ions measured in snow (Pearson's correlation of 0.99), indicating a common source. The ratio of Na and Cl in sea salt is well established and consistent globally (Pytkowicz and Kester, 1971). So, the measured relationships of these chemical species in the atmosphere and snow were compared to the expected marine ratio (Figure 3).

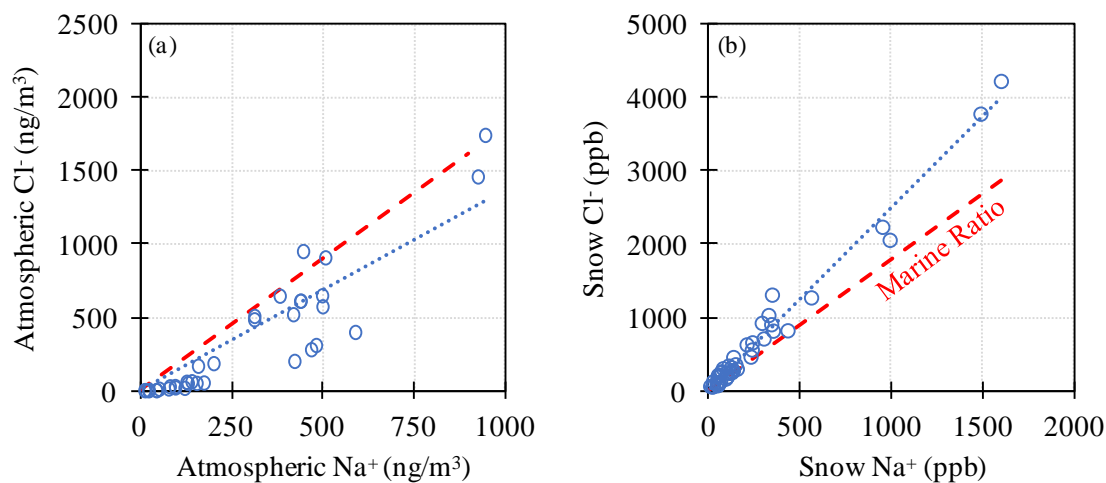


**Figure 3: Atmospheric (a) and snow (b) sea salt measurements. The marine ratio of  $\text{Cl}^-/\text{Na}^+$ , shown in red (1.795 mass/mass), is compared to the measured average ratios, shown in blue as the line of best fit, for atmospheric (slope=1.36, correlation=0.92) and snow measurements (slope=2.49, correlation=0.99).**

It was observed that while atmospheric particulate monitoring showed a deficit in Cl, snow samples showed an enhancement in Cl relative its marine ratio with Na. This discrepancy may be explained by partitioning of Cl from the particle to the gas phase, and subsequent gas-phase scavenging by snow. It has been suggested that Cl within Arctic aerosol will partition to the gas phase during the winter, likely in the form of HCl via acid displacement reactions; however, there is no similar evidence for Na being involved in analogous chemistry (Toom-Sauntry and Barrie, 2002). The gas-phase portion of Cl would not be captured by atmospheric particulate monitoring, causing a perceived deficit and reducing the correlation of Na and Cl if the gas-phase partitioning were non-linear. In contrast, gas-phase Cl deposited to the snowpack would be measured during snow analysis, leading to an increased Cl/Na ratio and an improved agreement between Cl and Na. The proportion of Cl in the atmosphere which partitioned to the gas phase was estimated from the observed atmospheric deficit below the marine ratio to



be approximately 24% by mass on average over the 2014-15 winter season (assuming a common marine origin of Na and Cl and that Na remains fully in the particle phase). In addition, the enhancement of Cl in snow above the marine ratio demonstrates that gas-phase Cl was preferentially deposited to the snow over the particle phase. Snow Cl scavenged from the particle phase was estimated from snow Na using the observed atmospheric Cl/Na ratio (1.36 mass/mass) and the remaining  
5 Cl in snow was considered to be scavenged from the gas phase. Based on these estimated gas and particle-phase proportions in the snow and atmosphere, median effective deposition velocities were calculated as 0.16 and 0.40 cm/s for the particle and gas phases, respectively. Comparison of these velocities indicates an 86% enhancement in gas-phase deposition relative to that of the particle phase.

The effective deposition velocities provided in Figure 2 showed BC to have the lowest median velocity. The velocities of  
10  $\text{NH}_4$ ,  $\text{SO}_4$ , Na, K, Mg,  $\text{C}_2\text{O}_4$ , and Ca showed enhancement relative to BC, though statistical significance could be shown only for  $\text{Ca}^{2+}$  using the ANOVA test (p-value 0.008) due to the low number of samples. Particles containing these analytes have been previously suggested to act as better precipitation nuclei than BC (e.g., Zobrist et al., 2006; Hoose and Möhler, 2012; Farmer, Cappa, and Kreidenweis, 2015), thus their enhanced velocities might be attributed to either enhanced scavenging via  
15 cloud formation or in-cloud scavenging. Furthermore, salt and crustal particles may experience enhanced deposition since they typically consist of coarser particles than BC,  $\text{SO}_4$ , and  $\text{NH}_4$ . Specifically, coarse mode particles can exhibit dry deposition velocities to snow up to 0.6 cm/s and below-cloud scavenging efficiencies enhanced over accumulation mode particles by a factor of 10 (Zhang and Vet, 2006; Petroff and Zhang, 2010). The observed difference in deposition velocities also implies that BC-containing particles are to a significant extent externally mixed from these other constituents. Gas-phase deposition to snow is suggested to contribute to the observed enhanced velocities of methanesulphonate (MSA), Br,  
20 Cl, and  $\text{NO}_3$  relative to BC, either due to gas-phase emissions or gas-phase partitioning during aerosol aging followed by subsequent deposition.

### 3.2.3 Temporal Variability of Deposition

Several factors controlling deposition experience seasonal variations, which may have contributed to the observed inter-monthly variability. Across the campaign months, a relative standard deviation of 60 to 180% was observed in deposition  
25 velocities. Figure 4 shows the range of effective deposition velocities normalized by their associated campaign average for all measured chemical species over the sampling campaign as well as the average seasonal trend (the seasonal trends of individual analytes are provided in the supplemental Figure S3). In general, higher velocities were observed in the fall and spring. The deposition velocities for January and February are low and may be underestimated due to the presumed loss of snow from the snow tables during these months.

30 Three properties of the Arctic system with seasonal trends were considered as possible influences on the observed velocity trend: precipitation, temperature, and dominant aerosol source region. The precipitated snow-water equivalent depth was calculated from the snow mass and table area of each sample and temperature monitored at local meteorological stations

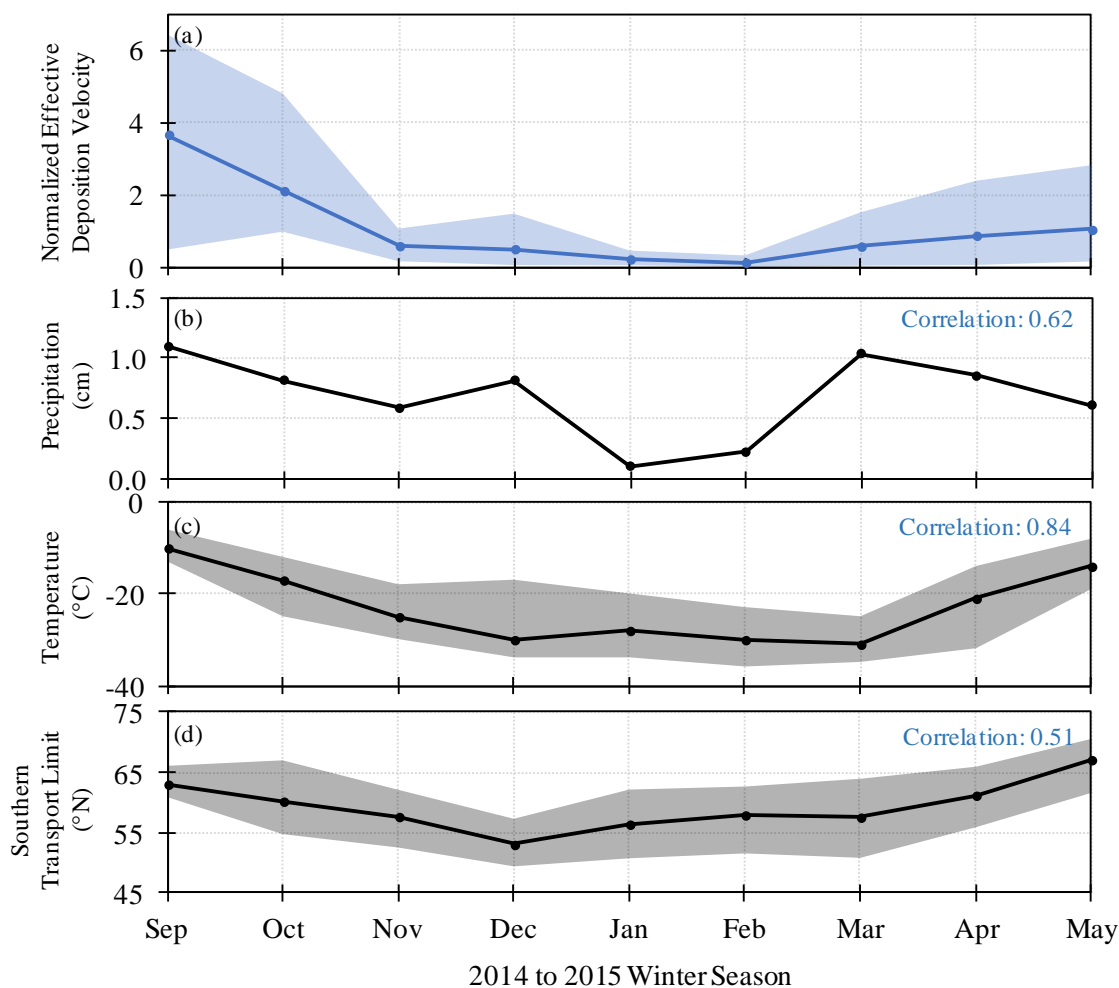


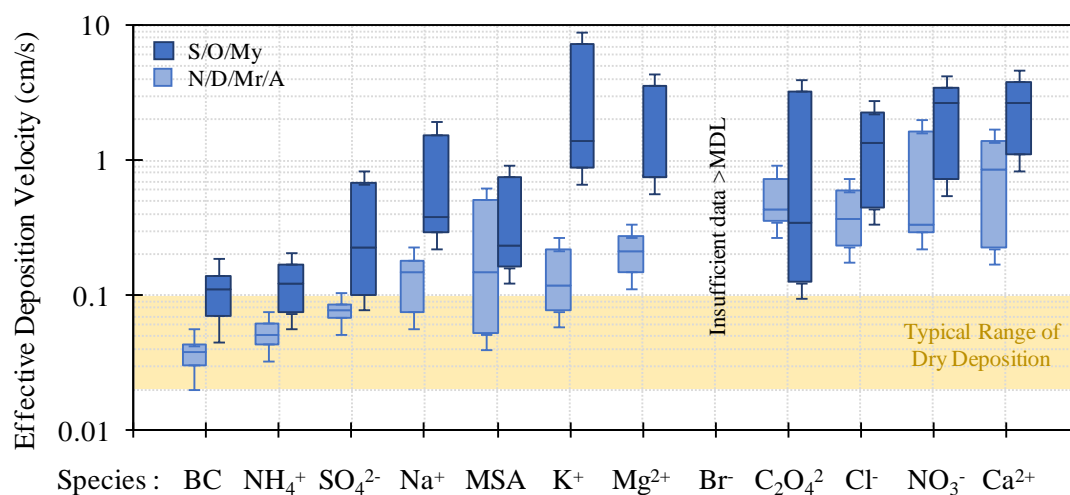
Figure 4: Seasonal variation in deposition velocity (a), precipitation (b), temperature (c), and transport (d). For velocity and temperature, the shaded areas show the range of observations over each month and the lines show the average monthly value. For precipitation, the total monthly depth is shown. For transport limit, the shaded area shows the range of average latitudes across the modelled receptor altitudes and the line shows the average transport limit. Correlations with the average normalized effective deposition velocity are provided.

over the campaign. The dominant aerosol source of each month was described using the southern limit to transport, calculated from the FLEXPART results as the latitude which encircles 98% of the 10-day transport source area and presented as a range based on initialization altitude (100 m, 500 m, 1 km, and 2km above Alert). The seasonal pattern of the average effective deposition velocity showed better agreement with the seasonal trend in temperature than with that of precipitation depth or transport limit, with Pearson's correlation coefficients of 0.8, 0.6, and 0.5, respectively (0.80, 0.52, and 0.44 if January and February are excluded) with p-values of 0.005, 0.08, and 0.16, respectively. Thus, changes in temperature may be linked to changes in the dominant scavenging mechanism. Specifically, it is hypothesized that the



increased presence of mixed-phase clouds with warmer temperatures may have enhanced wet deposition via in-cloud scavenging due to CCN activity.

The effective deposition velocities for warmer and colder months were separated using a  $-20\text{ }^{\circ}\text{C}$  cut-off between ice-cloud dominated periods, November to April (N/D/Mr/A), and months with a significant potential for mixed-phase clouds, September, October, and May (S/O/My). Comparison of the effective deposition velocities delineated by these periods minimized the influence of precipitation volume as it was relative constant: an average of 12 mm/month in S/O/My and 18 mm/month in N/D/Mr/A. However, the influence of aerosol source may differ by period given their distinct source profiles: long-range transport dominated in N/D/Mr/A, and local transport dominated in S/O/My. Figure 5 depicts the range of effective deposition velocities calculated for each analyte over these two periods (again excluding January and February). Bromide was excluded from this analysis since it was below detection limit in the snow and/or atmospheric measurements from September to November.



S/O/My Median : 0.11 0.12 0.23 0.37 0.24 1.36 0.76 n/a 0.34 1.34 2.66 2.67

N/D/Mr/A Median : 0.04 0.05 0.08 0.15 0.15 0.12 0.21 n/a 0.43 0.36 0.33 0.85

**Figure 5: Effective deposition velocities split by season. The effective deposition velocities are separated into two time periods: warmer months S/O/My = September/October/May, and colder months N/D/Mr/A = November/December/March/April.**

With the exception of C<sub>2</sub>O<sub>4</sub>, all analytes showed a larger median effective deposition velocity for the warmer S/O/My months than the colder N/D/Mr/A months. Although insufficient data are available to confirm the statistical significance for each individual analyte, the combined normalized dataset of velocities showed significant enhancement during S/O/My using the ANOVA test ( $p\text{-value } 4.9 \times 10^{-8}$ ). Specifically, marked enhancement was seen for BC, NH<sub>4</sub>, SO<sub>4</sub>, Na, K, and Mg. The cold-month deposition of these analytes can largely be described by dry deposition alone with velocities below 0.1 cm/s for analytes expected to be dominated by accumulation mode particles and 0.6 cm/s for those expected to include significant coarse-mode mass; however, their warm-month effective deposition velocities were a factor of 2 to 12 higher. This suggests



that these chemical species were preferentially scavenged during the warmer S/O/My months, possibly due to the presence of mixed-phase clouds and the associated CCN activation of these chemical species or enhanced below-cloud deposition of those associated with larger particles. However, the change in source profile typically experienced during these months along with other seasonal changes in aerosol processing and altitudinal distribution might have also contributed to the observed S/O/My enhancement. In particular, records of volcanic activity show that the Icelandic volcano Bárðarbunga was active August, 2014 through February, 2015 (Global Volcanism Program, retrieved March 2016 from <http://volcano.si.edu/>), which likely contributed a shift in the dominant source and scavenging-related properties of SO<sub>4</sub> over the campaign that would not be representative of a typical year. The overlapping warm/cold-month ranges observed for Cl, MSA, C<sub>2</sub>O<sub>4</sub>, and NO<sub>3</sub> suggest that the deposition of these chemical species was more strongly driven by factors other than nucleation, such as gas-phase partitioning or other aerosol aging processes. For example, enhanced deposition of MSA and Br<sup>-</sup> was observed as early as March and April, which could imply that their deposition was impacted by changes in the atmospheric processing of these chemical species during polar sunrise.

The enhanced deposition of Ca compared to the other particle-phase species is unexpected. Both Mg and Ca are common to sea salt and crustal origins but their non-sea salt (NSS) portions can be estimated based on typical sea salt ratios with Na (Pytkowicz and Kester, 1971). The NSS-Mg and NSS-Ca showed similar behaviour over the warm months, with average velocities of 2.4 and 2.6 cm/s, respectively, but a larger difference in the cold months, with average velocities of 0.4 and 1.0 cm/s, respectively. Assuming a crustal source with internally mixed aerosol these analytes would have been expected to show more similar velocities. No explanation of this discrepancy can be proposed without further study; however, the phenomenon may be connected to the dissimilar sources of Ca-rich mineral dust to that of other crustal species suggested by other studies (Banta et al., 2008).

#### 4 Conclusions

To help characterize the chemical state of the rapidly changing high Arctic, an intensive campaign of fresh snow sampling at Alert, Nunavut, was completed and snow quantified for a broad suite of analytes. Comparison of these snow measurements with coincident atmospheric measurements allowed estimation of monthly effective deposition velocities describing the total dry and wet deposition in the range of about 0.02 to 8 cm/s. The calculated effective deposition velocities for several measured chemical species resemble those expected for dry deposition alone, suggesting that dry deposition may be the dominant removal mechanism, especially for winter scavenging of BC, NH<sub>4</sub>, SO<sub>4</sub>, Na, and K. Enhanced deposition during September, October, and May suggests that wet deposition may increase in importance during these warmer months, possibly due to the presence of mixed-phase clouds and the associated scavenging of crustal, salt, and SO<sub>4</sub> species as CCN; however, other factors such as changes in the dominant aerosol source profile may also contribute to the observed trend. Comparison of salt species measurements in the Arctic snow and atmosphere suggested that Cl experiences significant gas-phase partitioning and that this gas phase material may be preferentially scavenged. Such gas-phase scavenging may





contribute to the enhanced deposition of MSA, Br, Cl, and NO<sub>3</sub> observed relative to BC, in conjunction with other aerosol processing differences. The low deposition efficiency of BC-containing particles is consistent with those particles being externally mixed from more soluble species and having a low cloud nucleation efficiency. Given the rarity of temporally-refined and broadly speciated Arctic snow sampling campaigns, measured deposition magnitudes and insights on deposition mechanisms such as these are valuable for future model validation.

### Author Contribution

Organization of the snow collection campaign was lead by S. Sharma with the assistance of A. Platt and sample collection by M. Elsasser. Snow SP2 analysis was completed by J. McConnell and N. Chellman, snow IC analysis lead by D. Toom with the assistance of A. Chivulescu, and snow ICP-MS by K. Macdonald with the assistance of Y. Lei. Ambient atmospheric monitoring of inorganic aerosols was completed by D. Toom and monitoring of BC by S. Hanna with the assistance of A. Bertram and Richard Leaitch. FLEXPART simulations were completed by H. Bozem and D. Kunkel with data analysis assisted by K. Macdonald. Data interpretation was led by K. Macdonald with input and comments by all authors. Dr. G. Evans and J. Abbatt provided oversight for the project, including input on the manuscript.

### Competing interests

The authors declare that they have no conflict of interest.

### Acknowledgements

Funding of this study was provided as part of the Network on Climate and Aerosols Research (NETCARE), Natural Science and Engineering Research Council of Canada (NSERC), the government of Ontario through the Ontario Graduate Scholarship (OGS), and Environment and Climate Change Canada. This project would not have been possible without the collaboration of many skilled individuals: Richard Leaitch at Environment Canada; and Catherine Philips-Smith and Cheol-Heon Jeong at the University of Toronto. In addition, the preview of Alert vertical profiles provided by Julia Burkart and Megan Willis, University of Toronto, was an excellent addition in the validation of assumptions in this work.

### References

AMAP: Snow, water, ice and permafrost in the Arctic: Climate change and the cryosphere, Arctic Monitoring and Assessment Programme, Oslo, Norway, 2011.



- Banta, J. R., McConnell, J. R., Edwards, R., and Engelbrecht, J. P.: Delineation of carbonate dust, aluminous dust, and sea salt deposition in a Greenland glaciochemical array using positive matrix factorization, *Geochem. Geophys. Geos.*, 9 (7), 1–19, doi:10.1029/2007GC001908, 2008.
- Bond, T. C., Doherty, S. J., Fahey, D. W., Forster, P. M., Berntsen, T., Deangelo, B. J., Flanner, M. G., et al.: Bounding the  
5 role of black carbon in the climate system: A Scientific assessment, *J. Geophys. Res.-Atmos.*, 118, 5380–5552, doi:10.1002/jgrd.50171, 2013.
- Davidson, C. I., Honrath, R. E., Kadane, J. B., Tsay, R. S., Mayewski, P. A., Lyons, W. B., and Heidam, N. Z.: The Scavenging of atmospheric sulfate by Arctic snow, *Atmos. Environ. A-Gen.*, 21 (4), 871–882, doi:10.1016/0004-6981(87)90083-7, 1987.
- 10 Farmer, D. K., Cappa, C. D., and Kreidenweis, S. M.: Atmospheric processes and their controlling influence on cloud condensation nuclei activity. *Chem. Rev.*, 115 (10), 4199–4217, doi:10.1021/cr5006292, 2015.
- Hartmann, D. J., Klein Tank, A. M. G., Rusticucci, M., Alexander, L. V., Brönnimann, S., Charabi, Y. A.-R., Dentener, F. J., et al.: Observations: Atmosphere and surface, *Climate change 2013: The Physical science basis, Contribution of working group I to the fifth assessment report of the Intergovernmental Panel on Climate Change [Stocker, T.F., D. Qin, G.-K.*  
15 *Plattner, M. Tignor, S.K. Allen, J. Boschung, A. Nauels, Y. Xia, V. Bex and P.M. Midgley (eds.)], Cambridge University Press, Cambridge and New York, NY, doi:10.1017/CBO9781107415324.008, 2013.*
- Henry, R. and Wills, J.: Drinking water compliance monitoring using US EPA method 200.8 with the Thermo Scientific iCAP Q ICP-MS (Application Note 43127 ), Thermo Scientific, 2012.
- Hillamo, R.E., Kerminen, V.-M., Maenhaut, W., Jaffrezo, J.-L., Balachandran, S., and Davidson, C.I.: Size distributions of  
20 atmospheric trace elements at Dye 3, Greenland: I. Distribution characteristics and dry deposition velocities, *Atmos. Environ. A-Gen.*, 27 (17), 2787–2802, doi:10.1016/0960-1686(93)90311-L, 1993.
- Hoose, C. and Möhler, O.: Heterogeneous ice nucleation on atmospheric aerosols: A Review of results from laboratory experiments, *Atmos. Chem. Phys.*, 12 (20), 9817–9854, doi:10.5194/acp-12-9817-2012, 2012.
- Law, K. S. and Stohl, A.: Arctic air pollution: Origins and impacts, *Science*, 315, 1537–1540, doi:10.1126/science.1137695,  
25 2007.
- Leitch, W. R., Hoff, R. M., and MacPherson, J. I.: Airborne and lidar measurements of aerosol and cloud particles in the troposphere over Alert Canada in April 1986, *J. Atmos. Chem.*, 9, 187–211, doi:10.1007/BF00052832, 1989.
- Macdonald, K.: The Chemical composition of high Arctic snow: Deposition mechanisms and sources, M.A.Sc. thesis, University of Toronto, ON, 2016.
- 30 McConnell, J. R., Edwards, R., Kok, G. L., Flanner, M. G., Zender, C. S., Saltzman, E. S., Banta, J. R., et al.: 20th-Century industrial black carbon emissions altered Arctic climate forcing, *Science*, 317, 1381–1384, doi:10.1126/science.1144856, 2007.
- McMahon, T. A. and Denison, P. J.: Empirical atmospheric deposition parameters: A Survey, *Atmos. Environ.* (1967), 13 (5), 571–585, doi:10.1016/0004-6981(79)90186-0, 1979.



- Morrison, H., Shupe, M. D., Pinto, J. O., and Curry, J.: Possible roles of ice nucleation mode and ice nuclei depletion in the extended lifetime of Arctic mixed-phase clouds, *Geophys. Res. Lett.*, 32 (18), 1–5, doi:10.1029/2005GL023614, 2005.
- Nguyen, Q. T., Skov, H., Sørensen, L. L., Jensen, B. J., Grube, A. G., Massling, A., Glasius, M., and Nøjgaard, J. K.: Source apportionment of particles at Station Nord, north east Greenland during 2008-2010 using COPREM and PMF analysis, *Atmos. Chem. Phys.*, 13, 35–49, doi:10.5194/acp-13-35-2013, 2013.
- Norris, G., Duvall, R., Brown, S., and Bai, S.: EPA Positive matrix factorization (PMF) 5.0 fundamentals and user guide, U.S. Environmental Protection Agency, 2014.
- Paatero, P. and Hopke, P. K.: Discarding or downweighting high-noise variables in factor analytic models, *Anal. Chim. Acta*, 490, 277–289, doi:10.1016/S0003-2670(02)01643-4, 2003.
- Paris, J.-D., Stohl, A., Nédélec, P., Arshinov, M. Y., Panchenko, M. V., Shmargunov, V. P., Law, K. S., et al.: Wildfire smoke in the Siberian Arctic in summer: Source characterization and plume evolution from airborne measurements, *Atmos. Chem. Phys. Discussions*, 9, 18201–18233, doi:10.5194/acpd-9-18201-2009, 2009.
- Pekney, N. J. and Davidson, C. I.: Determination of trace elements in ambient aerosol samples, *Anal. Chim. Acta*, 540 (2), 269–277, doi:10.1016/j.aca.2005.03.065, 2005.
- Petroff, A. and Zhang, L.: Development and validation of a size-resolved particle dry deposition scheme for application in aerosol transport models, *Geoscientific Model Development*, 3 (2), 753–769, doi:10.5194/gmd-3-753-2010, 2010.
- Pytkowicz, R. M. and Kester, D. R.: The Physical chemistry of sea water, *Oceanogr. Mar. Biol.*, 9, 11–60, doi:10.1029/WR001i002p00263, 1971.
- Quinn, P. K., Shaw, G., Andrews, E., Dutton, E. G., Ruoho-Airola, T., and Gong, S. L.: Arctic haze – Current trends and knowledge gaps, *Tellus B.*, 59 (1), 99–114, doi:10.1111/j.1600-0889.2006.00238.x, 2007.
- Reff, A., Eberly, S. I., and Bhave, P. V.: Receptor modeling of ambient particulate matter data using positive matrix factorization: Review of existing methods, *Journal of the Air and Waste Management Association* (1995), 57 (August 2014), 146–154, doi:10.1080/10473289.2007.10465319, 2007.
- Rigor, I. G., Colony, R. L., and Martin, S.: Variations in surface air temperature observations in the Arctic: 1979-97, *J. Climate*, 13 (5), 896–914, doi:10.1175/1520-0442(2000)013<0896:VISATO>2.0.CO;2, 2000.
- Schroder, J. C., Hanna, S. J., Modini, R. L., Corrigan, A. L., Kreidenwies, S. M., MacDonald, A. M., Noone, K. J., et al.: Size-resolved observations of refractory black carbon particles in cloud droplets at a marine boundary layer site, *Atmos. Chem. Phys.*, 15 (3), 1367–1383, doi:10.5194/acp-15-1367-2015, 2015.
- Sehmel, G. A.: Particle and gas dry deposition: A Review, *Atmos. Environ.* (1967), 14 (9), 983–1011, doi:10.1016/0004-6981(80)90031-1, 1980.
- Seinfeld J. H., and Pandis, S. N.: Atmospheric chemistry and physics – From Air pollution to climate change, Wiley, Michigan, USA, 2006.



- Sharma, S., Ishizawa, M., Chan, D., Lavoué, D., Andrews, E., Eleftheriadis, K., and Maksyutov, S.: 16-Year simulation of Arctic black carbon: Transport, source contribution, and sensitivity analysis on deposition, *J. Geophys. Res.-Atmos.*, 118, 943–964, doi:10.1029/2012JD017774, 2013.
- Shupe, M. D., Matrosov, S. Y., and Uttal, T.: Arctic mixed-phase cloud properties derived from surface-based sensors at SHEBA, *J. Atmos. Sci.*, 63 (2), 697–711, doi:10.1175/JAS3659.1, 2006.
- Sirois, A. and Barrie, L. A.: Arctic lower tropospheric aerosol trends and composition at Alert, Canada: 1980–1995, *J. Geophys. Res.*, 104 (D9), 11599–11618, doi:10.1029/1999JD900077, 1999.
- Spackman, J. R., Gao, R. S., Neff, W. D., Schwarz, J. P., Watts, L. A., Fahey, D. W., Holloway, J. S., et al.: Aircraft observations of enhancement and depletion of black carbon mass in the springtime Arctic, *Atmos. Chem. Phys.*, 10, 9667–9680, doi:10.5194/acp-10-9667-2010, 2010.
- Stohl, A., Forster, C., Frank, A., Seibert, P., and Wotawa, G.: Technical note – The Lagrangian particle dispersion model FLEXPART version 6.2, *Atmos. Chem. Phys.*, 5(9), 2461–2474, doi:10.5194/acp-5-2461-2005, 2005.
- Stroeve, J. C., Serreze, M. C., Fetterer, F., Arbetter, T., Meier, W., Maslanik, J., and Knowles, K.: Tracking the Arctic’s shrinking ice cover: another extreme September minimum in 2004, *Geophys. Res. Lett.*, 32 (4), 1–4, doi:10.1029/2004GL021810, 2005.
- Swami, K., Judd, C. D., Orsini, J., Yang, K. X., and Husain, L.: Microwave assisted digestion of atmospheric aerosol samples followed by inductively coupled plasma mass spectrometry determination of trace elements, *Fresen. J. Anal. Chem.*, 369 (1), 63–70, doi:10.1007/s002160000575, 2001.
- Toom-Saunty, D. and Barrie, L. A.: Chemical composition of snowfall in the high Arctic: 1990 – 1994, *Atmos. Environ.*, 36, 2683–2693, doi:10.1016/S1352-2310(02)00115-2, 2002.
- US EPA: EPA Method 3015A: Microwave assisted acid digestion of aqueous samples and extracts, Rev. 1, U.S. Environmental Protection Agency, 2007.
- Wang, Y. and Miao, J.: iCAP Qc-ICPMS 用于 GB5749-2006 标准饮用水中的 重金属杂质元素分析 (Application Notes\_C\_ICPMS-8) (Translation: iCAP Qc-ICPMS for GB5749-2006 Standard - Heavy metal impurity elements in drinking water analysis), ThermoFisher Scientific: China, 2016.
- Zhang, L. and Vet, R.: A Review of current knowledge concerning size-dependent aerosol removal, *China Part.*, 4 (6), 272–282, doi:10.1016/S1672-2515(07)60276-0, 2006.
- Zobrist, B., Marcolli, C., Koop, T., Luo, B. P., Murphy, D. M., Lohmann, U., Zardini, A., et al.: Oxalic acid as a heterogeneous ice nucleus in the upper troposphere and its indirect aerosol effect, *Atmos. Chem. Phys.*, 6, 3115–3129, doi:10.5194/acpd-6-3571-2006, 2006.